

Electronic Supplementary Information

Dual-response NIR probe reveal positive correlation between biothiols and viscosity under cellular stress change

Sha Li,^a Fangjun Huo,^{b*} Ying Wen^a and Caixia Yin^{a*}

^a Key Laboratory of Chemical Biology and Molecular Engineering of Ministry of Education, Key Laboratory of Materials for Energy Conversion and Storage of Shanxi Province, Institute of Molecular Science, Shanxi University, Taiyuan 030006, China.

*E-mail: yincx@sxu.edu.cn

^b Research Institute of Applied Chemistry, Shanxi University, Taiyuan 030006, China.

Table of contents

1. Experimental section

2. Supplemental figures

Figure S1: The characterization data of NIR-2/NIR-NBD.

Figure S2: ESIMS analysis of NIR-NBD+thiols.

Figure S3: UV-Vis absorption spectra of NIR-NBD towards Cys/Hcy/GSH and viscosity.

Figure S4: Plot of the fluorescence intensity of NIR-NBD as a function of Cys/Hcy/GSH and viscosity.

Figure S5: The fluorescence intensity of NIR-NBD with Cys/Hcy/GSH and other amino acids (10 equiv).

Figure S6: Different pH values fluorescent changes of NIR-NBD in the absence and present of thiols and time response of NIR-NBD with thiols.

Figure S7: Cytotoxicity assay of NIR-NBD at different concentration for HeLa and HepG-2 cells.

Figure S8: Construction of oxidative stress: Images of biomeraptan in HeLa cells stimulated by PEICT at different concentrations.

Figure S9: Construction of oxidative stress: Images of biomeraptan in HepG-2 cells stimulated by ROT at different concentrations.

Figure S10: Construction of oxidative stress: Images of biomeraptan in HepG-2 cells stimulated by PEICT at different concentrations.

Figure S11: Fluorescence images of NIR-NBD for Cys, Hcy and GSH in living zebrafish.

Figure S12: Construction of oxidative stress: Images of biothiols in zebrafish stimulated by PEITC at different concentrations.

Figure S13: Fluorescence imaging of viscosity in HeLa cells.

Figure S14: Construction of inflammation model: Images of viscosity in HeLa cells stimulated by LPS at different times.

1. EXPERIMENTAL SECTION

1.1 Materials and instruments

All chemicals from Aladdin were used without further purification. Fluorescence spectra were carried out a HITACHI F-7000 spectrophotometer. UV-visible spectra were recorded with a HITACHI U-3900 spectrophotometer. NMR spectra were recorded on a JBruker AVANCE-600MHz spectrometer and chemical shifts were referenced relative to tetramethylsilane. Mass data (ESI) were obtained by an AB Triple TOF 5600 plus System (AB SCIEX, Framingham, USA). The final bioimaging application were measured by the Zeiss LSM 880 Airyscan confocal laser scanning microscope.

1.2 Synthesis of NIR-Q

A synthetic route for compound NIR-Q from commercially available compounds was provided and depicted in Scheme 1. Compound NIR-1 was synthesized according to refs 32.

4-methylquinoline (160.0 mg, 1.12 mmol) was dissolved in anhydrous DMF (10 mL), then benzoyl chloride (80.0 mg, 0.56 mmol) was added and stirred at room temperature for 30 min. After that, compound NIR-2 (130.0 mg, 0.56 mmol) was added and the mixture was reflux at 160°C for 5 h. After the reaction was complete, the reaction mixture was cooled to room temperature, diluted with H₂O and extracted with ethyl acetate (20 mL*3). The combined organic layer was washed with saturated sodium thiosulfate solution and dried with dry Na₂SO₄. the solid was obtained after the solvent was removed under reduced pressure and purified by column chromatography to obtain the product NIR-Q (100 mg, 65%).

1.3 Synthesis of NBD-Br

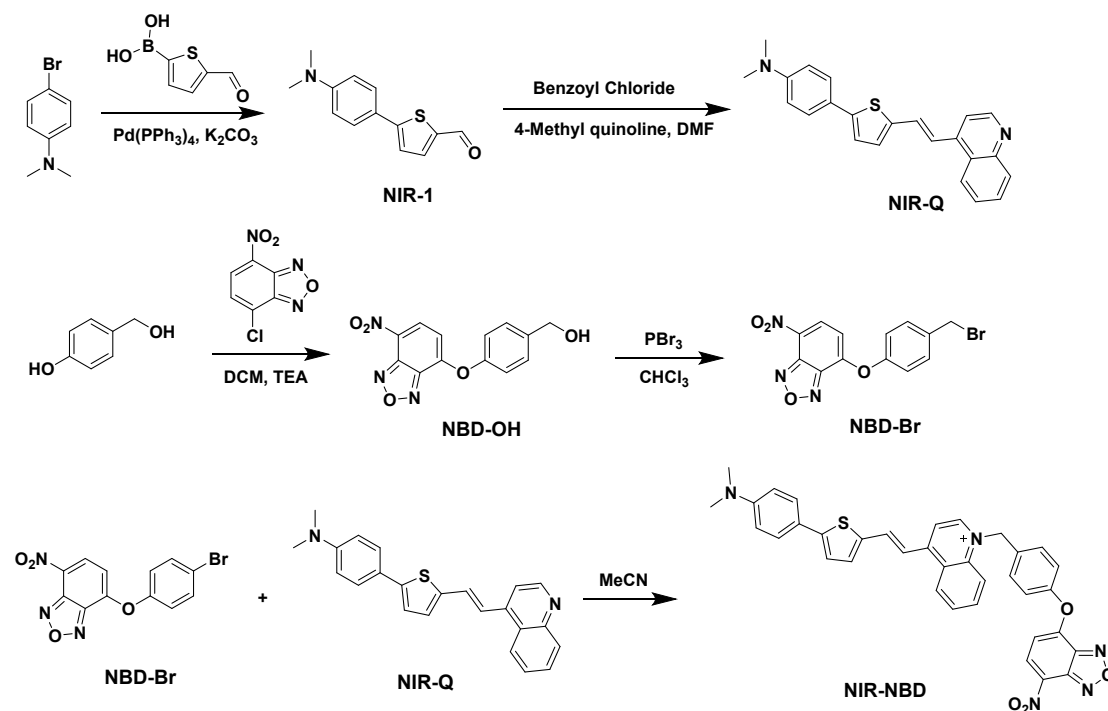
NBD-Cl (99.8 mg, 0.5 mmol) was dissolved in DCM (15 mL). After stirring in ice bath for 5 min, 4-hydroxybenzyl alcohol (62.07 mg, 0.5 mmol) dissolved in 10 mL DCM was added in batches. Then 200 microl triethylamine was added and the reaction was complete for 8 h. After decompression, the solvent was removed and purified by silica gel column chromatography to obtain the NBD-OH (60 mg, 60%).

NBD-OH (0.718 g, 2.5mmol) was dissolved in chloroform (20 mL) in a nitrogen atmosphere, and phosphorus tribromide (0.8 g, 3 mmol) was added in drops at room temperature. The mixture was stirred overnight at room temperature. After the reaction was complete, the solvent was removed by decompression and purified by silica gel column chromatography to obtain the NDB-Br (0.65 g, 90%).

1.4 Synthesis of NIR-NBD

NIR-Q (150 mg, 0.42 mmol) and NBD-Br (147 mg, 0.42 mmol) were added to acetonitrile (5 mL) solution. The reaction mixture was stirred to reflux. After the reaction was complete, the solvent was removed by decompression and purified by silica gel column chromatography to obtain the **NIR-NBD** (60 mg, 40%). ¹H NMR (600 MHz, DMSO) δ 9.51 (d, *J* = 6.6 Hz, 1H), 8.99 (d, *J* = 8.6 Hz, 1H), 8.65 (d, *J* = 8.3 Hz, 1H), 8.52 (t, *J* = 10.6 Hz, 2H), 8.42 (d, *J* = 8.9 Hz, 1H), 8.19 (t, *J* = 7.8 Hz, 1H), 7.99 (t, *J* = 7.7 Hz, 1H), 7.95-7.91 (m, 1H), 7.76 (d, *J* = 3.9 Hz, 1H), 7.62 (dd, *J* = 8.4, 3.8 Hz, 4H), 7.53 (d, *J* = 3.8 Hz, 1H), 7.46 (d, *J* = 8.5 Hz, 2H), 6.80 (d, *J* = 8.6 Hz, 2H), 6.69 (d, *J* = 8.3 Hz, 1H), 6.29 (s, 2H), 3.00 (s, 6H). ¹³C NMR (150 MHz,

DMSO) δ 167.75 (s), 153.62 (s), 153.48 (s), 153.12 (s), 151.55 (s), 151.19 (s), 147.91 (s), 145.84 (s), 144.84 (s), 138.49 (s), 138.12 (s), 137.69 (s), 135.90 (d, $J = 12.7$ Hz), 135.62 (s), 133.50 (s), 133.31 (s), 131.01 (s), 130.17 (s), 129.71 (s), 129.48 (s), 129.02 (s), 127.46-127.43 (m), 127.28 (d, $J = 25.0$ Hz), 126.89 (s), 123.39 (s), 121.81 (s), 121.43 (s), 119.80 (s), 116.79 (s), 115.80 (s), 112.83 (d, $J = 4.0$ Hz), 110.58 (s), 58.61 (s), 55.38 (s). HRMS: $[M-I]^+$ Calcd. For 626.1857; Found 626.1860.



Scheme S1 Synthesis of probe **NIR-NBD**.

HRMS characterization of **NIR-NBD**+Cys/Hcy and GSH were measured. **NIR-NBD** reacts with GSH to produce the corresponding products NBD-GSH and NIR-Q, m/z : [NBD-GSH] Calcd 469.0783; Found 469.0785. After Cys/Hcy treatment, the products are NBD-Cys/NBD-Hcy and NIR-Q, m/z : [NBD-Cys] Calcd 283.0143; Found 283.0144; [NBD-Hcy] Calcd 297.0299; Found 297.0301.

The three biothiols showed good linearity in the concentration range of 0.05-100.0 μM . The regression equation was $y=385.952+14.594$ [Cys], $R^2=0.995$, the detection limit (LOD, $S/N=3$) was calculated to be 0.063 μM ; $y=283.667+43.35$ [Hcy], $R^2=0.993$, LOD=0.053 μM ; $y=487.190+5.373$ [GSH], $R^2=0.997$, LOD=0.079 μM .

1.5 the biological section

(1) Cell culture and imaging

HeLa cells and HepG2 cells were cultured in 1640 medium (added with 12% fetal bovine serum and 1% double antibody) in a 37 $^\circ\text{C}$, 5% CO_2 incubator. When the cells were in logarithmic growth phase, they were seeded in 96 wells Plates or six-well plates with coverslips placed for 24 h.

Probe (10 μM) was dissolved in 2 mL of PBS, then added to confocal dishes

seeded with HeLa cells and HepG2 cells and incubated at 37°C for 20 min. In the detection of oxidative stress cells, HeLa cells and HepG2 cells loaded with probe were incubated with ROT and PEITC (0-10 μM) in PBS at 37°C for 20 min, and then the cells were washed with 2 mL of PBS for two days. After several times, perform cell imaging again. In the cell adhesion assay, probe was incubated with HeLa cells pretreated with nystatin and monensin (10 μM) in PBS at 37°C for 20 min, and then washed with 2 mL of PBS. After two times, the cells were imaged again. In the experiment of constructing an inflammatory cell model, HeLa cells loaded with probe were incubated with LPS (1 $\mu\text{g}/\text{mL}$) in PBS at 37°C for 20 min, and then the cells were washed twice with 2 mL of PBS, Cells were imaged over time. In the experiment to detect the relationship between cell thiols and viscosity, HeLa cells were first incubated with NEM (80 μM) in PBS at 37°C for 30 min, and then incubated with thiols and nystatin for 20 min, respectively, and then loaded with probe, after washing the cells twice with 2 mL of PBS before imaging the cells.

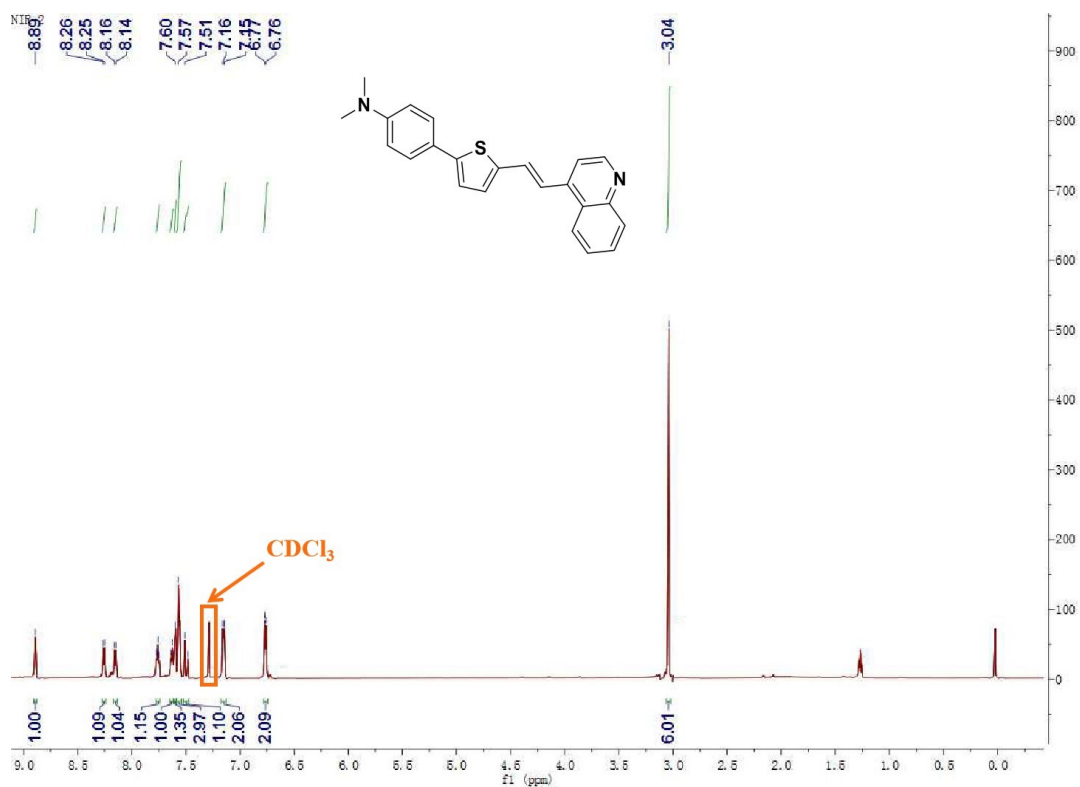
Real-time co-staining imaging: HeLa cells were washed three times with PBS in a confocal culture dish, incubated with PBS containing 500 μM Mito-Tracker Green for 15 min, and incubated with PBS containing 10 μM probe for 20 min, followed by three-channel fluorescence imaging.

(2) Zebrafish culture and imaging

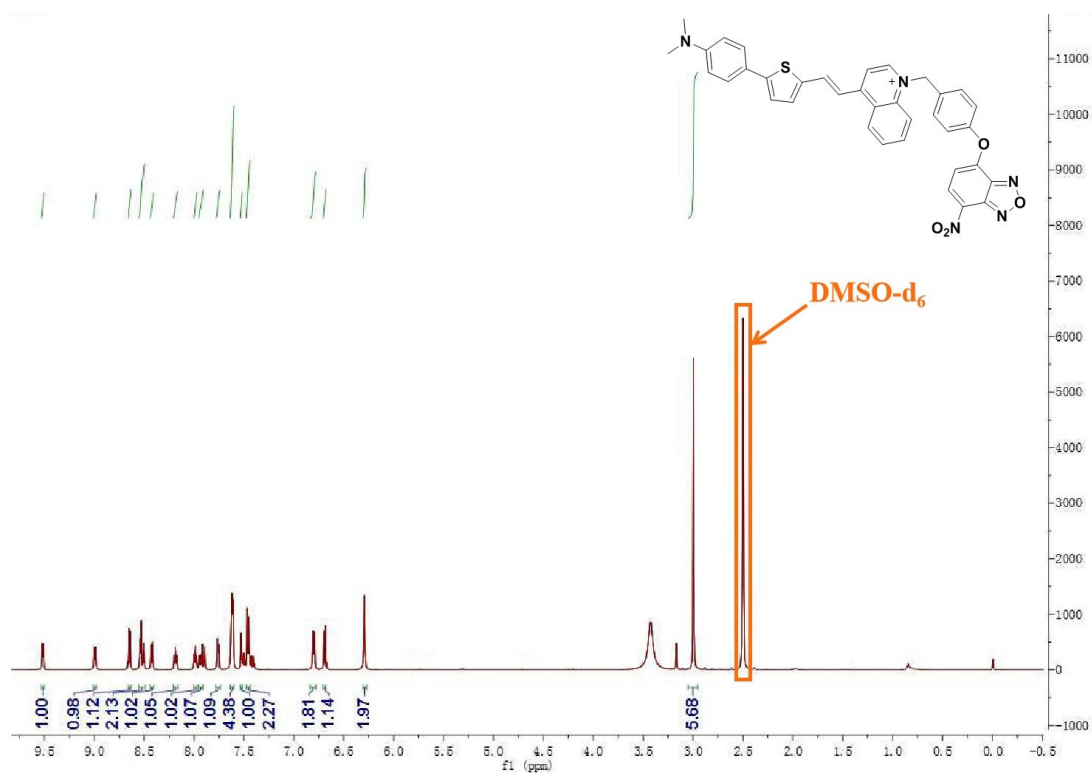
5-day-old zebrafish were incubated in E3 embryo medium containing 10 μM probe (15 mM NaCl, 0.5 mM KCl, 1 mM MgSO_4 , 1 mM CaCl_2 , 0.15 mM KH_2PO_4 , 0.05 mM Na_2HPO_4 , 0.7 mM NaHCO_3 , After 20 min incubation at 28°C in 5% methylene blue; pH 7.5), the zebrafish were anesthetized for imaging after three washes with PBS.

Another 5-day-old zebrafish was incubated with probe (10 μM) in E3 embryo medium at 28°C for 20 min, washed three times with PBS, and then added 100 μM Cys, Hcy, GSH and incubated for 20 min. After three washes with PBS, the zebrafish were anesthetized for imaging.

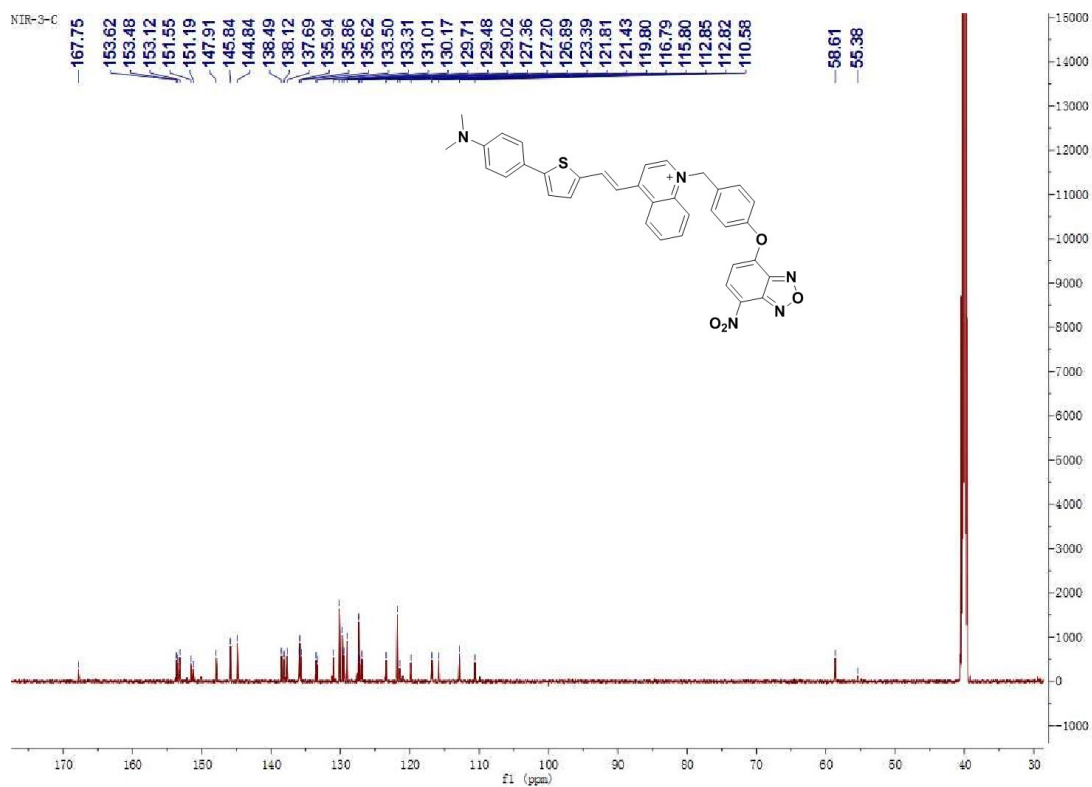
Another 5-day-old zebrafish was incubated in E3 embryo medium containing ROT and PEITC (0-10 μM) for 20 min at 28°C, washed three times with PBS, and incubated with PBS containing 10 μM probe for 15 min, washed three times with PBS, and zebrafish were anesthetized for imaging.



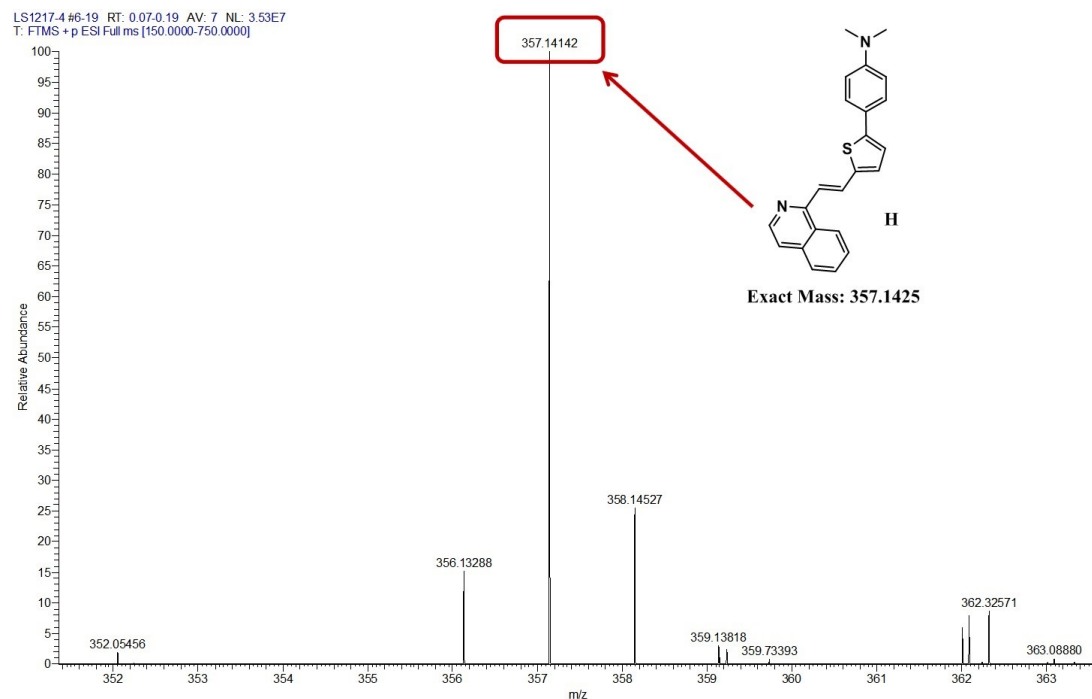
¹H NMR (600 MHz) of NIR-Q in CDCl₃



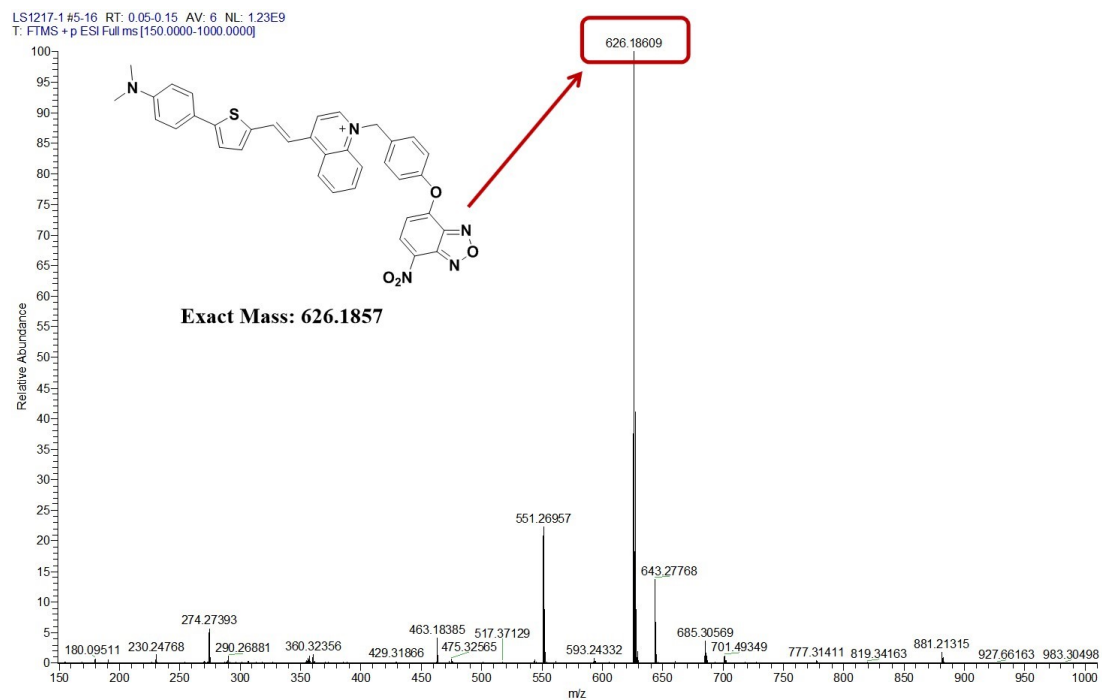
¹H NMR (600 MHz) of NIR-NBD in DMSO-d₆



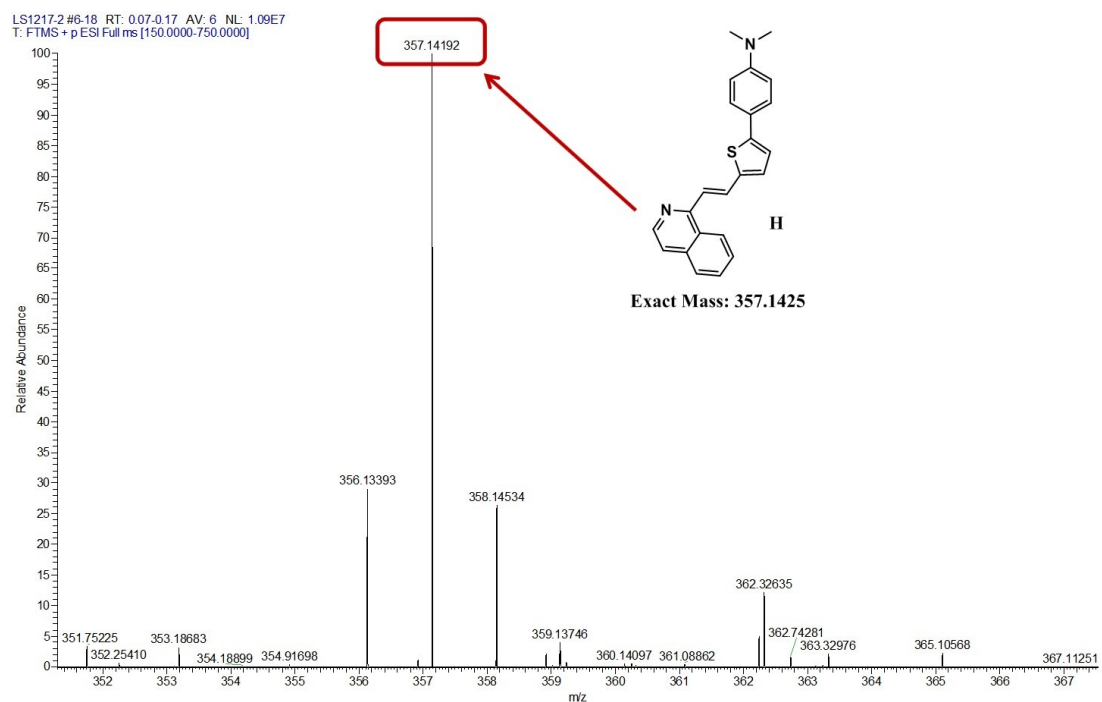
^{13}C NMR (150 MHz) of NIR-NBD in $\text{DMSO-}d_6$



HRMS spectra of NIR-Q

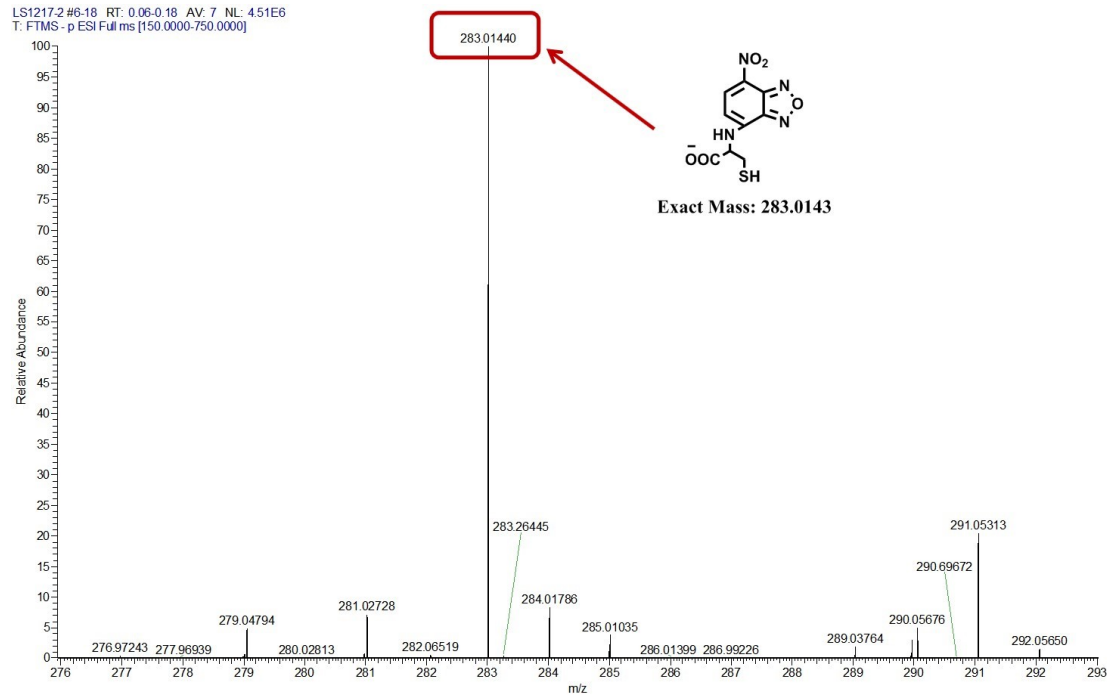


HRMS spectra of NIR-NBD
Figure S1. The characterization data of NIR-Q/NIR-NBD.



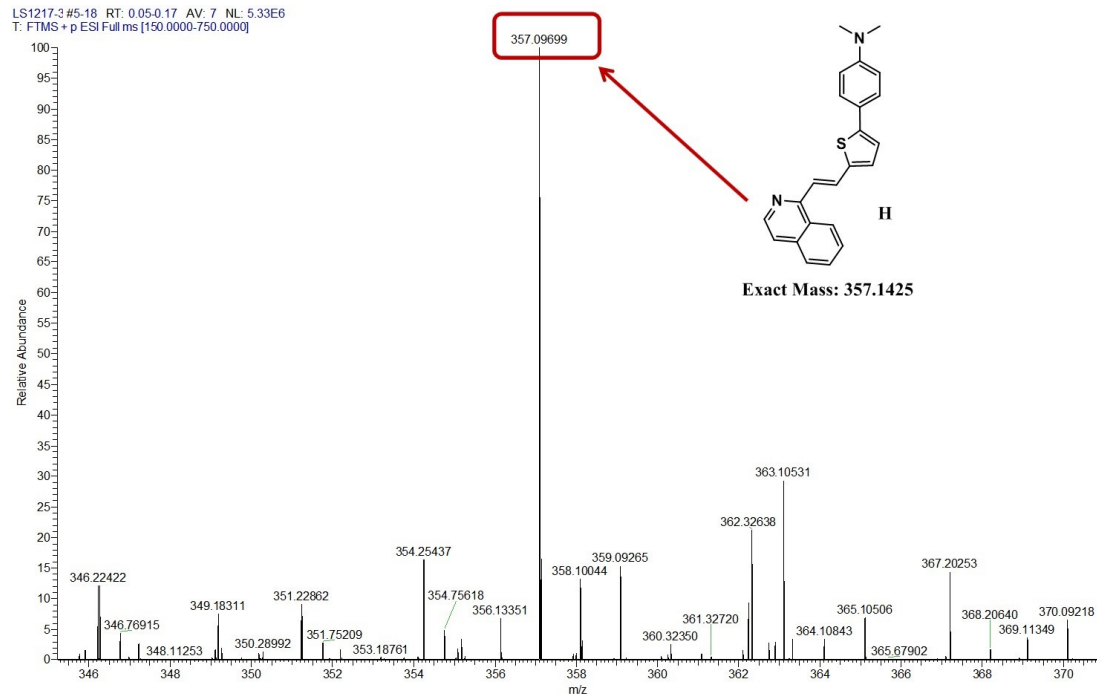
(a1) HRMS spectra of NIR-NBD +Cys

LS1217-2 #6-18 RT: 0.06-0.18 AV: 7 NL: 4.51E6
T: FTMS - p ESI Full ms [150.0000-750.0000]



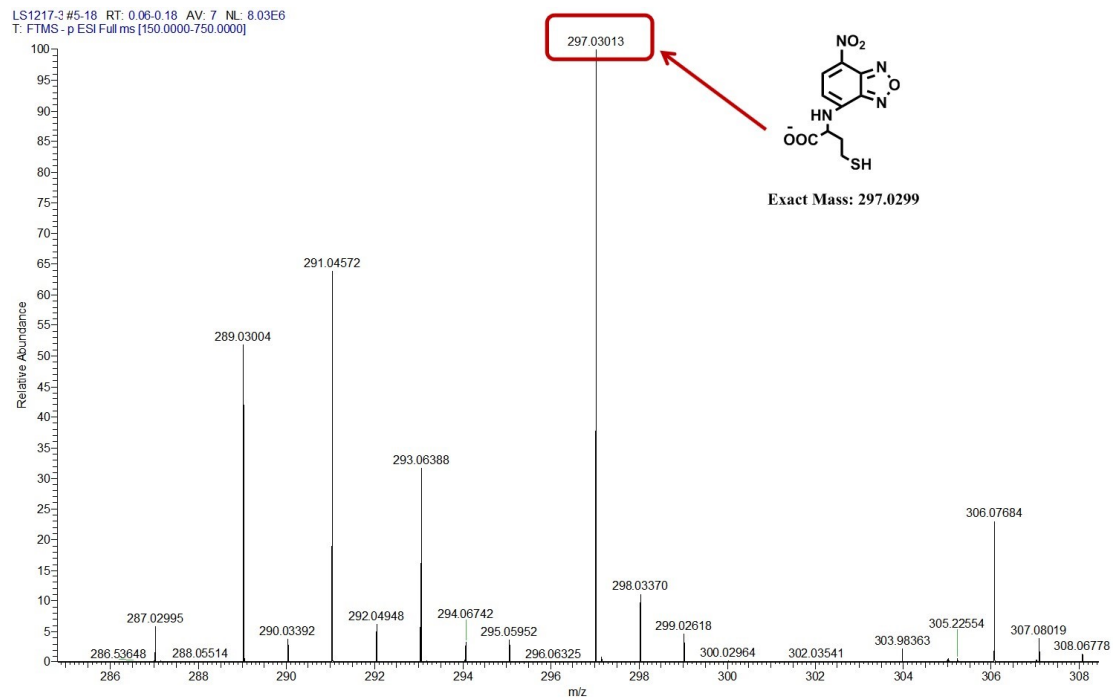
(a2) HRMS spectra of NIR-NBD +Cys

LS1217-3 #5-18 RT: 0.05-0.17 AV: 7 NL: 5.33E6
T: FTMS + p ESI Full ms [150.0000-750.0000]

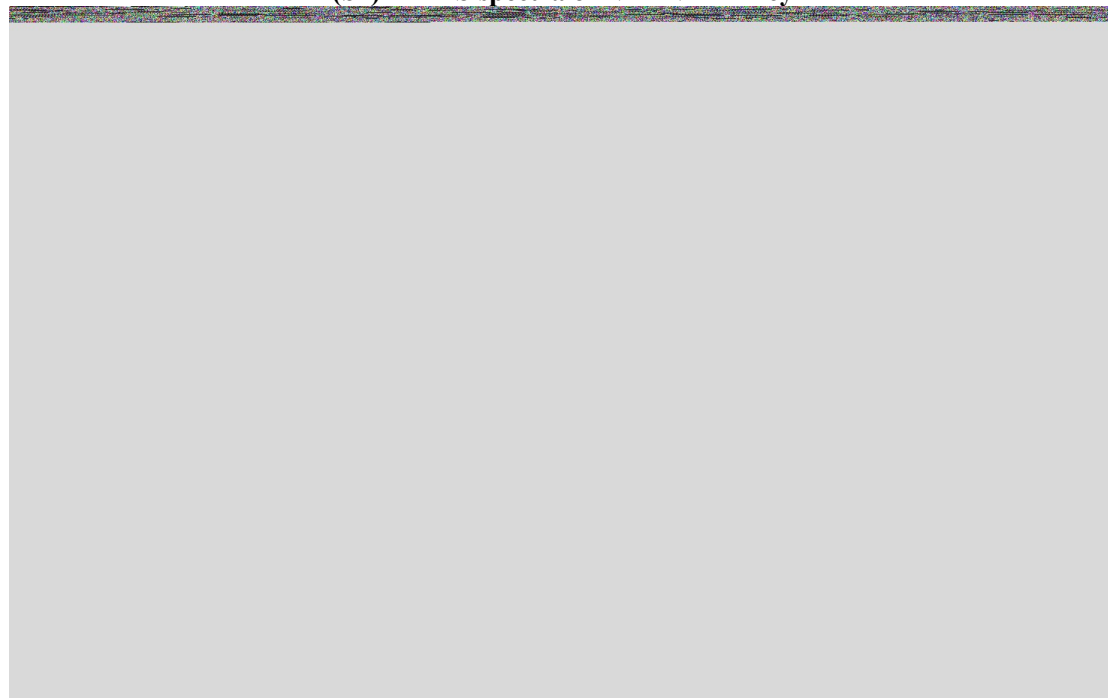


(b1) HRMS spectra of PI-CO-NBD +Hcy

LS1217-3 #5-18 RT: 0.06-0.18 AV: 7 NL: 8.03E6
T: FTMS - p ESI Full ms [150.0000-750.0000]

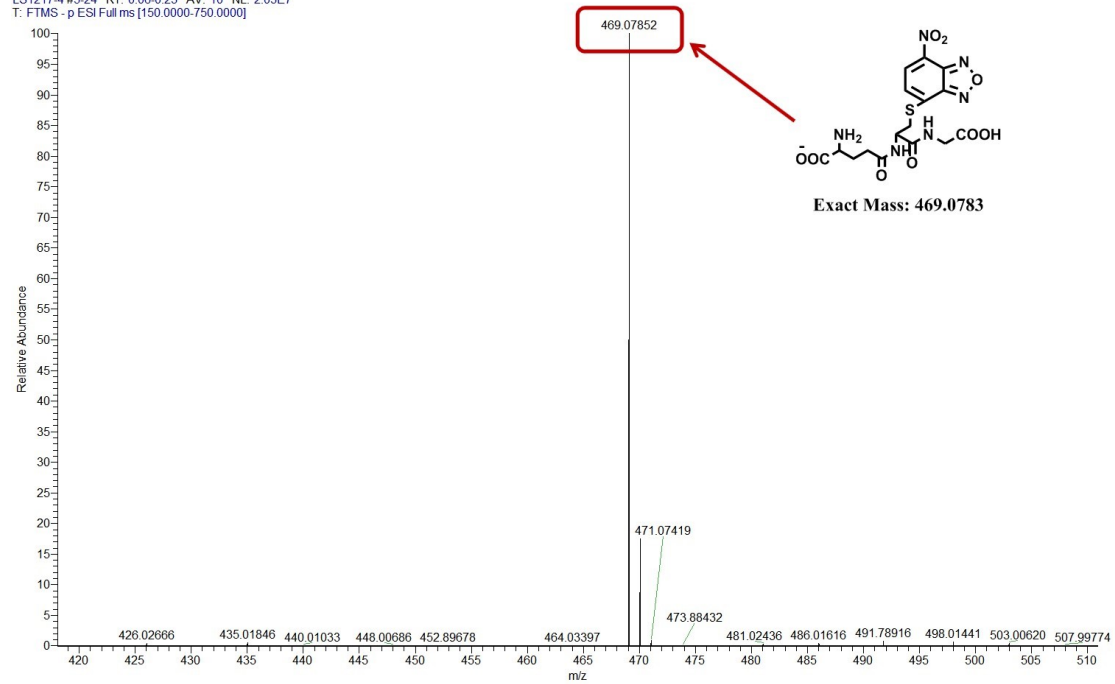


(b2) HRMS spectra of NIR-NBD +Hcy



(c1) HRMS spectra of NIR-NBD +GSH

LS1217-4 #5-24 RT: 0.06-0.23 AV: 10 NL: 2.03E7
T: FTMS - p ESI Full ms [150.0000-750.0000]



(c2) HRMS spectra of NIR-NBD +GSH

Figure S2 HRMS analysis of probe NIR-NBD+ thiols.

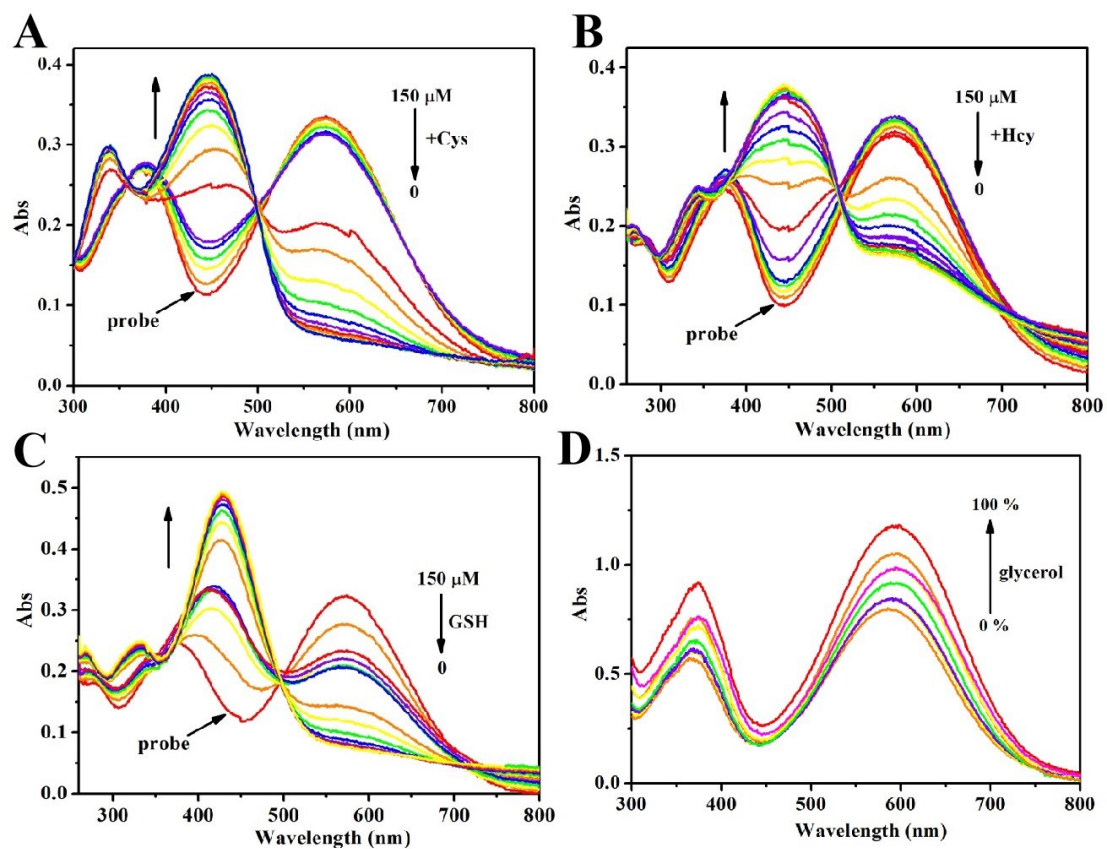


Figure S3. (A-C) UV-Vis absorption spectra of **NIR-NBD** (10 μM) towards Cys/Hcy/GSH in the PBS buffer (pH 7.4, containing 30% DMSO, v/v). (D) UV-Vis absorption spectra for viscosity in different volume ratios MeOH-glycerol solution.

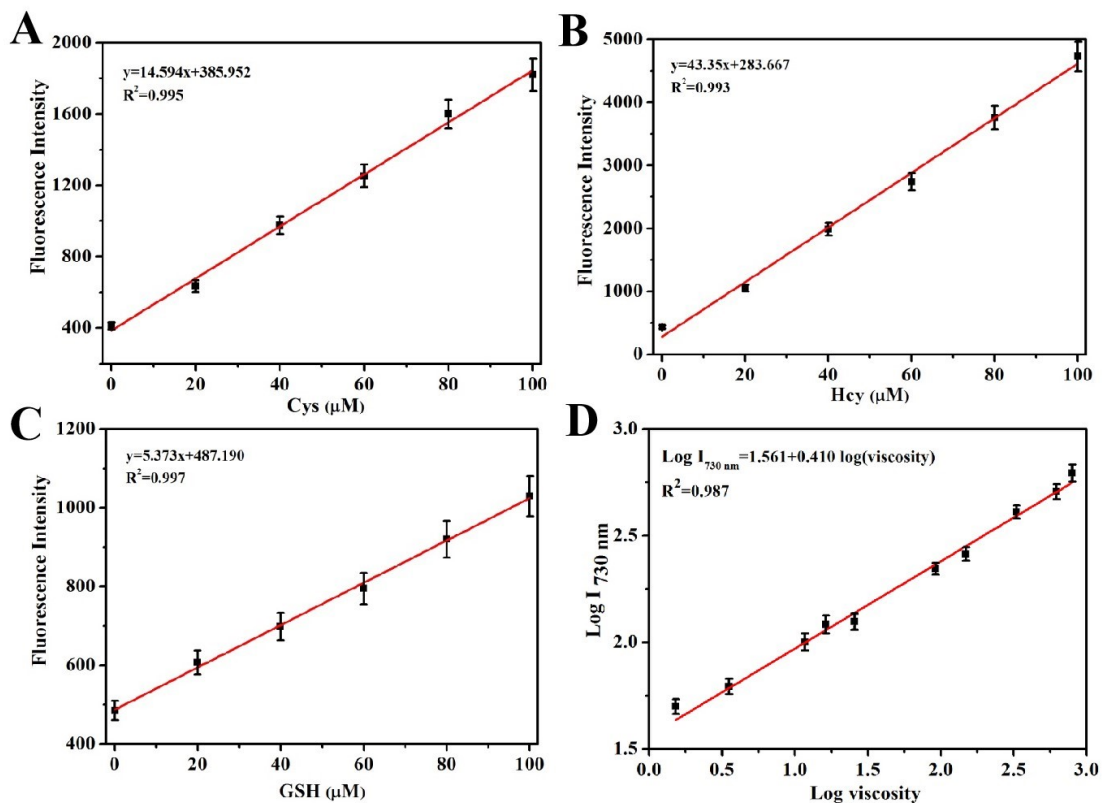


Figure S4. (A-C) Plot of the fluorescence intensity of NIR-NBD as a function of the Cys, Hcy and GSH. (D) Linear relationship between $\log(I_{730 \text{ nm}})$ and $\log(\text{viscosity})$

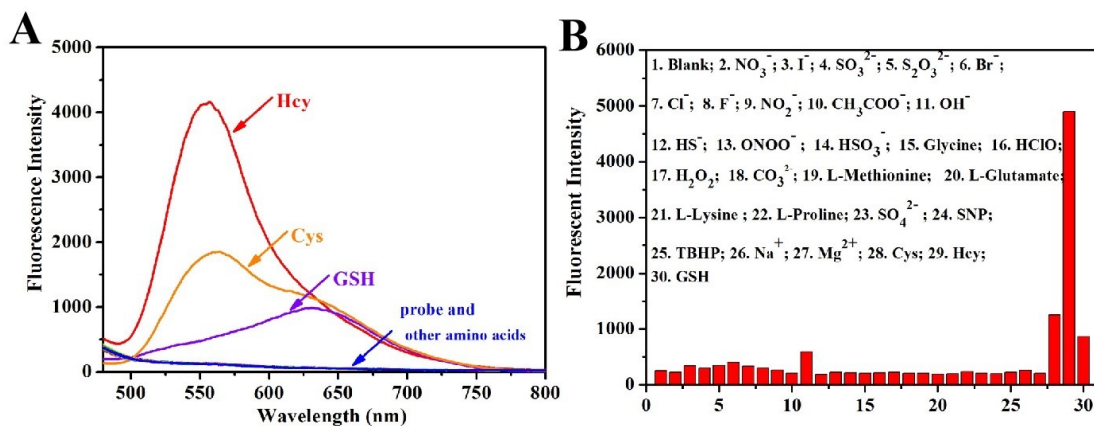


Figure S5. The fluorescence intensity of NIR-NBD ($10 \mu\text{M}$) with Cys/Hcy/GSH and other amino acids (10 equiv) in the PBS buffer (pH 7.4, containing 30% DMSO, v/v). $\lambda_{\text{ex}}=440 \text{ nm}$, Ex/Em slit: 5/5 nm.

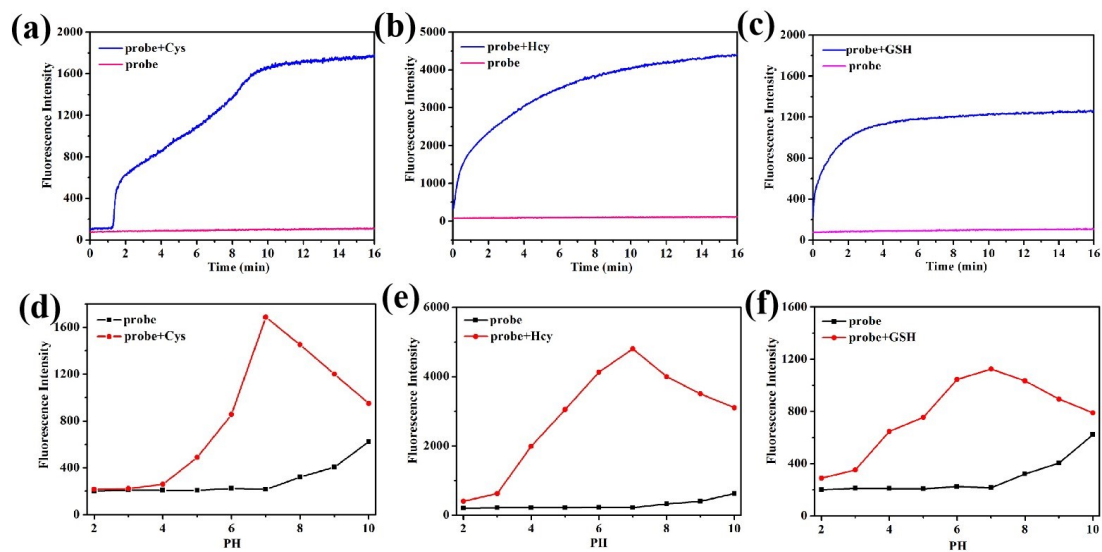


Figure S6. (a-c) Time response of NIR-NBD with thiols; (d-f) Different pH values fluorescent changes of NIR-NBD in the absence and present of thiols.

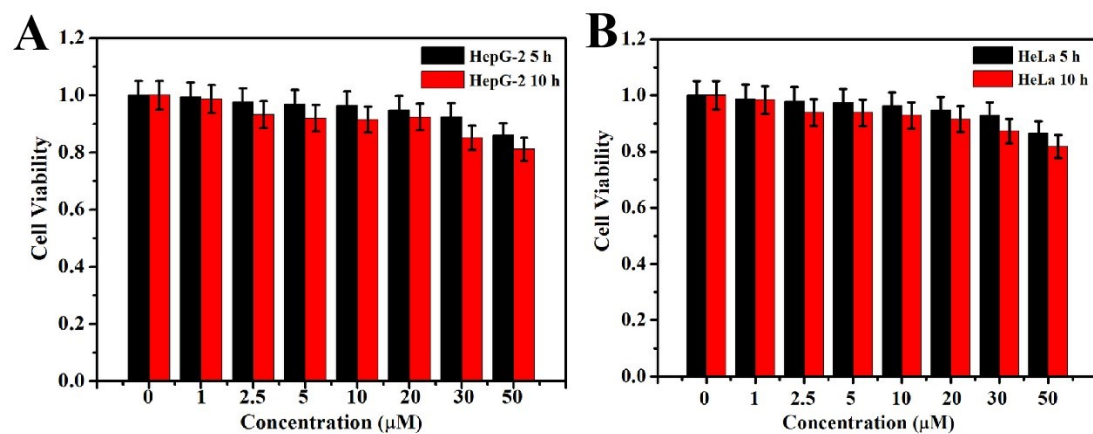


Figure S7. Cytotoxicity assay of probe NIR-NBD at different concentration for HeLa and HepG-2 cells.

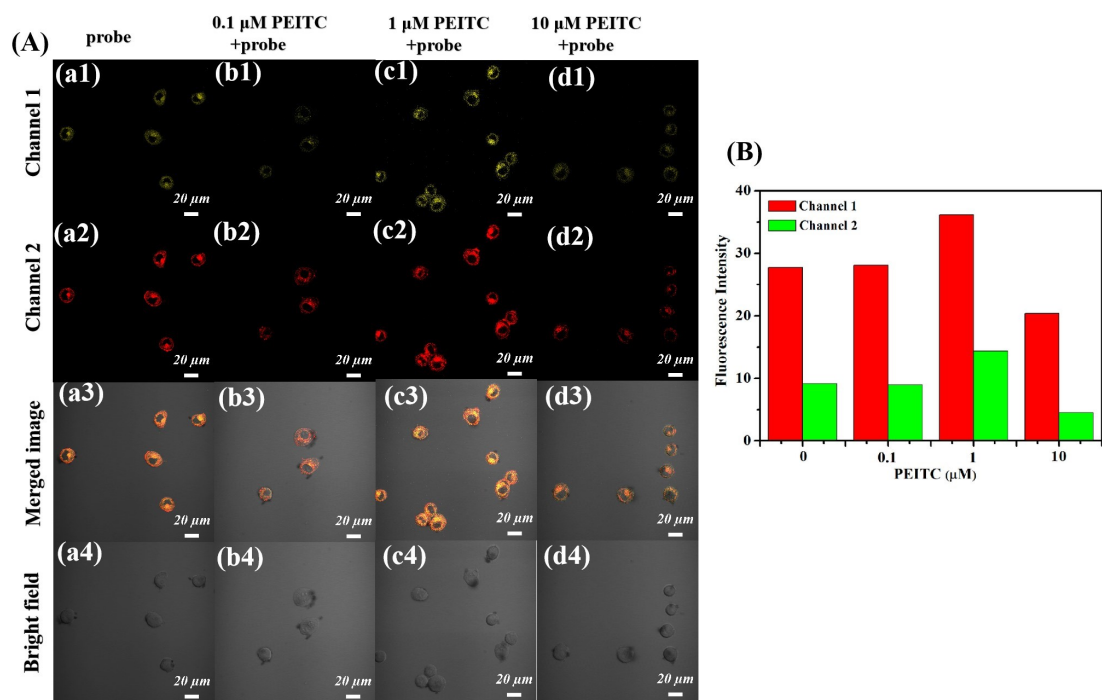


Figure S8. Construction of oxidative stress: Images of biothiols in HeLa cells stimulated by PEITC at different concentrations. (a1–d1): Channel 1 ($\lambda_{\text{ex}}=488$ nm and λ_{em} range 530–590 nm). (a2–d2): Channel 2 ($\lambda_{\text{ex}}=561$ nm and λ_{em} range 620–680 nm). (a3–d3): the merge images of Channel 1, 2 and Bright field. (a4–d4): the bright field image. Scale bar: 20 μm .

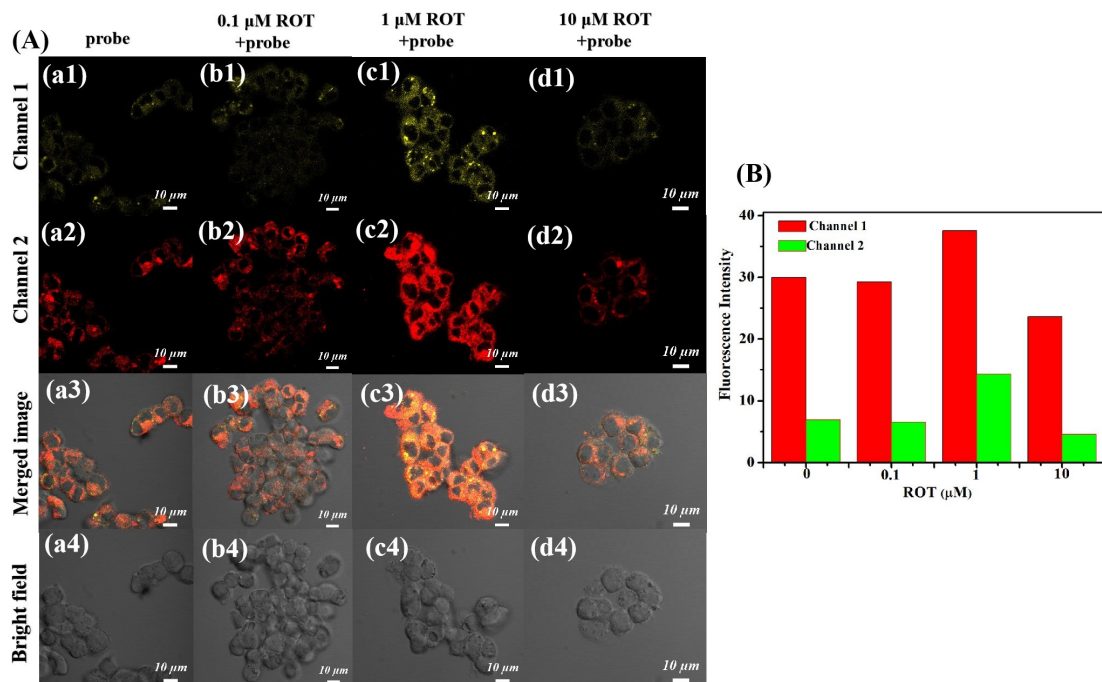


Figure S9. Construction of oxidative stress: Images of biothiols in HepG-2 cells stimulated by ROT at different concentrations. (a1–d1): Channel 1 ($\lambda_{\text{ex}}=488$ nm and λ_{em} range 530–590 nm). (a2–d2): Channel 2 ($\lambda_{\text{ex}}=561$ nm and λ_{em} range 620–680 nm). (a3–d3): the merge images of Channel 1, 2 and Bright field. (a4–d4): the bright field image. Scale bar: 10 μm .

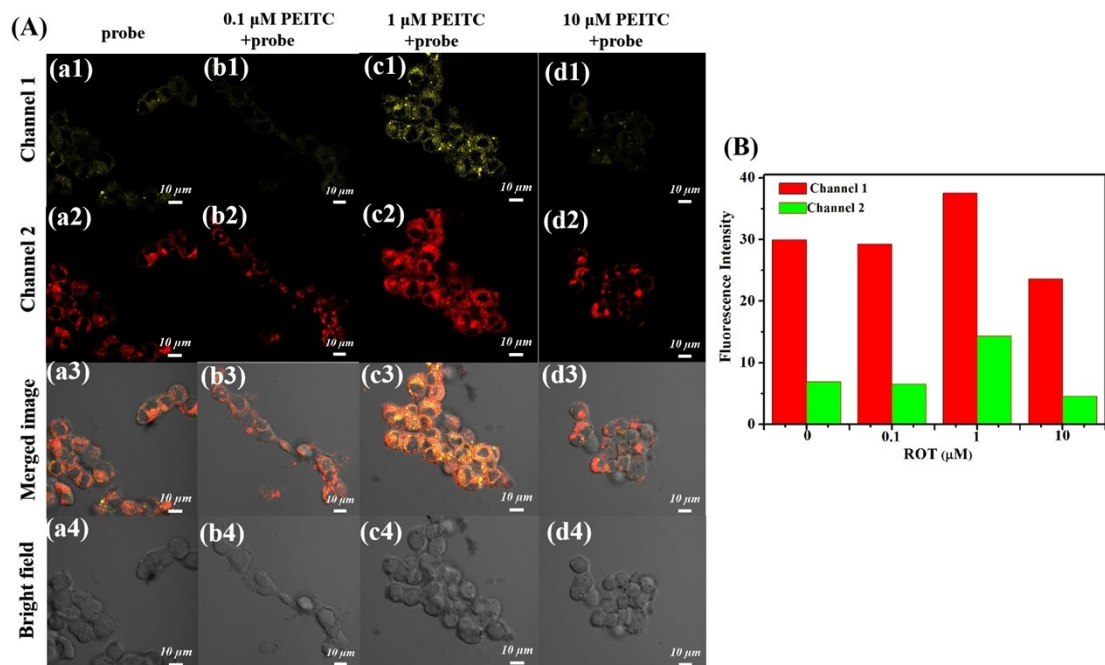


Figure S10. Construction of oxidative stress: Images of biothiols in HepG-2 cells stimulated by PEICT at different concentrations. (a1–d1): Channel 1 ($\lambda_{\text{ex}}=488$ nm and λ_{em} range 530–590 nm). (a2–d2): Channel 2 ($\lambda_{\text{ex}}=561$ nm and λ_{em} range 620–680 nm). (a3–d3): the merge images of Channel 1, 2 and Bright field. (a4–d4): the bright field image. Scale bar: 10 μm .

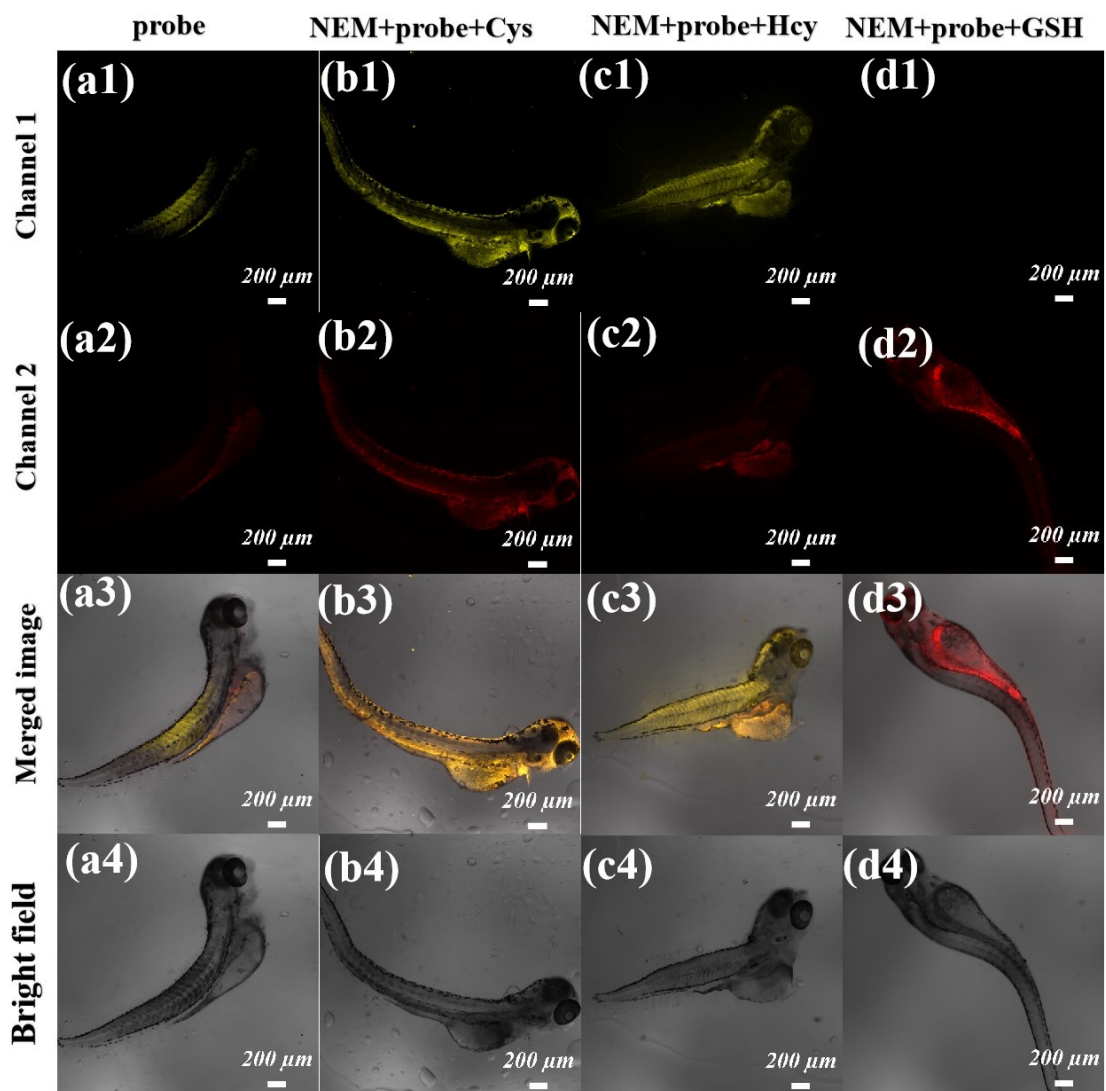


Figure S11. Fluorescence images of NIR-NBD for Cys, Hcy and GSH in living zebrafish. (a1–d1): Channel 1 ($\lambda_{\text{ex}}=488$ nm and λ_{em} range 530–590 nm). (a2–d2): Channel 2 ($\lambda_{\text{ex}}=561$ nm and λ_{em} range 620–680 nm). (a3–d3): the merge images of Channel 1, 2 and Bright field. (a4–d4): the bright field image. Scale bar: 200 μm .

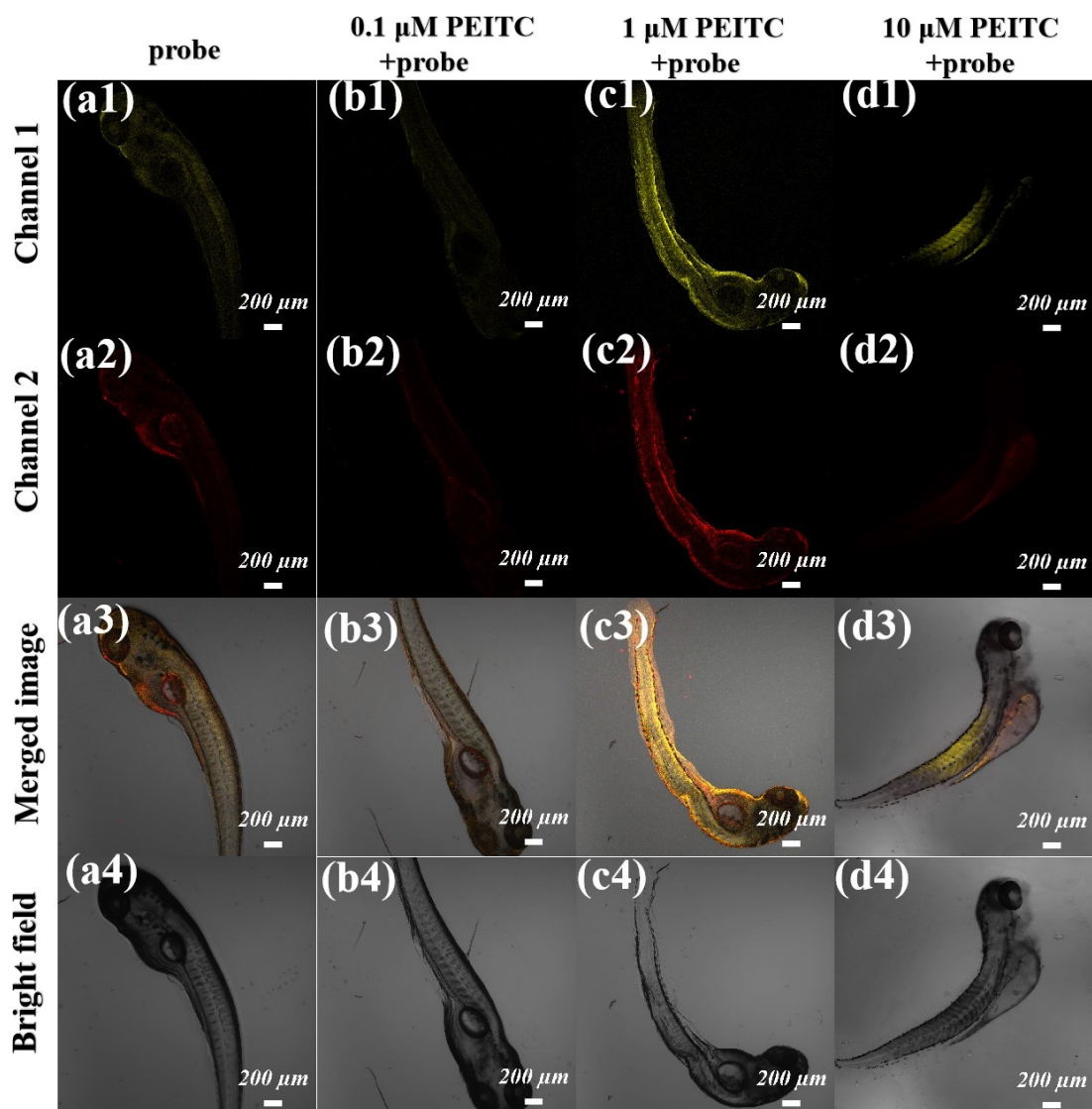


Figure S12. Construction of oxidative stress: Images of biothiols in zebrafish stimulated by PEITC at different concentrations. (a1–d1): Channel 1 ($\lambda_{\text{ex}}=488$ nm and λ_{em} range 530–590 nm). (a2–d2): Channel 2 ($\lambda_{\text{ex}}=561$ nm and λ_{em} range 620–680 nm). (a3–d3): the merge images of Channel 1, 2 and Bright field. (a4–d4): the bright field image. Scale bar: 200 μm .

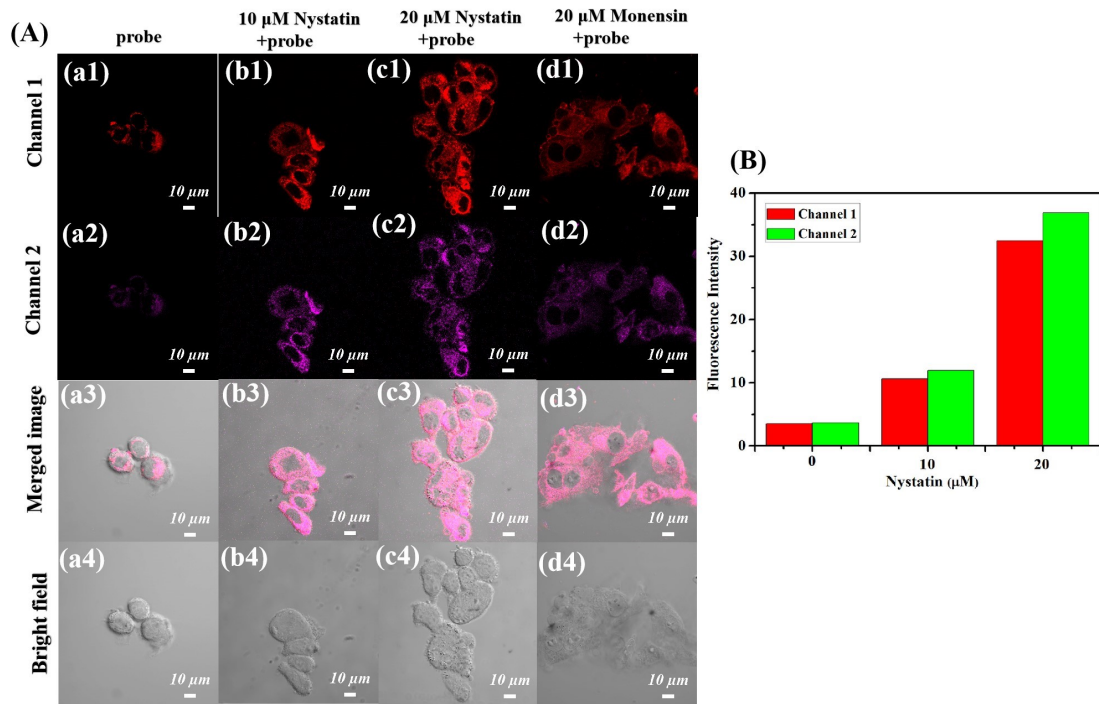


Figure S13. Fluorescence imaging of viscosity in HeLa cells. (a1–d1): Channel 1 ($\lambda_{\text{ex}}=561$ nm and λ_{em} range 620–680 nm). (a2–d2): Channel 2 ($\lambda_{\text{ex}}=633$ nm and λ_{em} range 700–760 nm). (a3–d3): the merge images of Channel 1, 2 and Bright field. (a4–d4): the bright field image. Scale bar: 10 μ m.

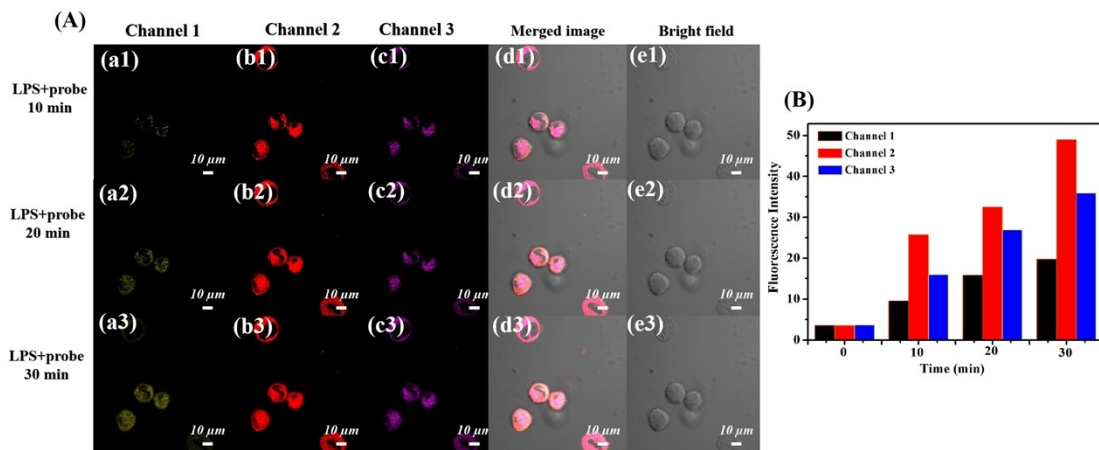


Figure S14. Construction of inflammation model: Images of viscosity in HeLa cells stimulated by LPS at different times. (a1–a3): Channel 1 ($\lambda_{\text{ex}}=488$ nm and λ_{em} range 530–590 nm). (b1–b3): Channel 2 ($\lambda_{\text{ex}}=561$ nm and λ_{em} range 620–680 nm). (c1–c3): Channel 3 ($\lambda_{\text{ex}}=633$ nm and λ_{em} range 700–760 nm). (d1–d3): the merge images of (a), (b), (c) and (e). (e1–e3): the bright field image. Scale bar: 10 μ m.